JOURNAL OF MATERIALS SCIENCE 23 (1988) 1817–1824

Effect of composition on the fracture strength of hot-pressed silicon nitride

J. E. O. OVRI, T. J. DAVIES
University of Manchester/UMIST, Department of Metallurgy and Materials Science, Grosvenor Street, Manchester M1 7HS, UK

The hot-pressing behaviour and fracture of silicon nitride as a function of composition was investigated. Two compositions were studied: 95 wt% Si_3N_4 + 5 wt% MgO, Material A, and 88 wt% Si_3N_4 + 2 wt% MgO + 10 wt% Y_2O_3, Material B. The effect of composition, hot-pressing time and temperature on the properties of the product were examined. The room-temperature fracture strengths of the two materials were evaluated using the diametral-compression disc test.

1. Introduction

Silicon nitride is a prime candidate material for certain high-temperature components of the gas turbine engine and other engineering applications [1–3]. The basic interest in this material is due in part to its strength retention at elevated temperatures, good thermal shock resistance and chemical stability [1]. However, fabrication of components in silicon nitride often presents difficulties which are thought to be related to it covalent bonding; the lack of diffusive processes to provide material transport for densification has led to the use of various densification aids to remove porosity. Densification aids are not always beneficial (in terms of achieving good mechanical properties) because these aids often solidify as glasses on grain boundaries in the silicon nitride; at elevated temperatures these glasses soften and this leads to strength degradation.

The relation between densification (or alternatively, pore removal), the fraction and composition on the glass phase and mechanical strength are reported in this paper.

Although the fracture strength of ceramic materials is often evaluated using the bend flexture test (three or four-point) it has been realized that this test provides only a partial characterization of the load-bearing capacity of such materials because the stress distribution in bending is not uniform, varying from zero at the neutral axis to a maximum at the outer surface, this is likely to accentuate the effects of surface condition on the measured fracture strength [1]. In the work reported here, the diametral-compression disc test was used in preference to the bend flexure test because this test avoids many of the problems associated with the specimen specification for the bend test [1].

2. Experimental procedures

2.1. Materials

2.1.1. Silicon nitride (SN6S)

The starting powders were manufactured by Denki Kagaku Kogyo K.K., West Germany and supplied by Turner and Newall Materials Research Limited, Trafford Park, Manchester after a pretreatment. The particle size distribution was determined experimentally using a Sedigraph (Model 500ET) and the results are shown in Table I. The specific surface area was also determined experimentally and a value of $6.7\,m^2\,g^{-1}$ was obtained. The spectrographic analysis of the minor elements of the starting powders is also given in Tables Ia to c.

2.2. Fabrication and physical examination

2.2.1. Hot-pressing

Discs of nominal dimensions 12.70 mm diameter and 6.35 mm thick ($\frac{1}{2}$ in. × $\frac{1}{4}$ in.) were hot-pressed in a graphite punch and die assembly in the temperature range 1450 to 1700° C for periods ranging from 3 to 40 min using high-frequency induction heating. The powders were initially cold-pressed in a steel die to about 55% of the theoretical density before hot-pressing. A pressure of 14 MPa ($14\,MN\,m^{-2}$) was applied uniaxially via the graphite plunger to the preformed compact. It was standard practice to apply only one-half of the ultimate pressure to the compact while the temperature was increased to 1250/1350° C because the onset of densification usually occurred in this temperature range; then applied pressure was gradually increased to the final pressure at 1450, 1550, 1650 or 1700° C, as required.

The interior of the graphite die was coated with boron nitride to inhibit interfacial reactions. The graphite die was inductively heated using a Radyne (G270/A9904) generator. Temperatures were measured using Pt–6%Rh/Pt–30% Rh thermocouples.

2.2.2. Physical examination techniques

The densities of the hot-pressed samples were measured using the Archimedes' method. The densities of porous material were determined after coating the surface with nitro-cellulose lacquer. Microstructural examinations were made on representative materials using a Philips EM301 transmission electron microscope (TEM) whilst macrohardness measurements

0022-2461/88 $03.00 + .12

TABLE I (a) Characterization of the starting powders. Elemental chemical analysis (wt %) (manufacturer's data

Element	Weight %
Si	59.5
N	38.5
Fe	0.28
Al	0.18
Ca	0.12
Mg	< 0.01

TABLE I (b) Spectrographic analysis of minor elements in the starting powders

Trace element	Material	
	A (wt %)	B (wt %)
Ca	–	–
Mg	1.11	–
Al	0.58	1.49
Si	–	–
Ti	–	–
Fe	0.23	0.07
Mn	–	–
Ni	0.15	0.17
Cr	–	1.23
Cu	0.08	0.11

TABLE I (c) Particle-size distribution

Diameter (μm)	Weight %
+ 10	0.3
10–8	1.3
8–5	6.8
5–3	16.8
3–2	13.5
– 2	61.5

were made using a Vickers diamond indentor with a 5 kg load.

2.3. Fracture strength

Fracture strength measurements were carried out at room temperature in air using an Instron machine (model TT-AO675) at a constant cross-head displacement rate of 0.2 mm min^{-1}.

3. Results

3.1. Effect of hot-pressing time on hot-pressed densities (1650 ± 20° C) at a pressure of 14 MPa

Table IIa contains the results of a selection of silicon nitride samples hot pressed in graphite dies at 14 MPa and 1650 ± 20° C; these results are plotted in Fig. 1. The densification rate was gradual for Material B for the first 5 min and then increased rapidly to about 98% theoretical density after 40 min. For Material A, densification was more rapid for the first 5 min (density of 90% theoretical was achieved after 5 min hot pressing) and the density increased steadily to about 97% theoretical density after 35 min. The density decreased slightly by extending the hot-pressing time to 40 min.

3.1.2. Densification results

The densification results for the hot-pressed silicon nitride samples are given in Table II and displayed in Figs 2 and 3. Fig. 2 is a plot of $\log_{10}(1-\varrho)$ against hot-pressing time using the modified hot-pressing equation [1, 2]

$$\log_{10}(1-\varrho) = -Kpt + \log_{10}(1-\varrho_0) \quad (1)$$

where ϱ and ϱ_0 are, respectively, the relative densities at $t > t_0$ and $t = 0$, p is the externally applied

TABLE II (a) Effect of time on the densities and macrohardness of material hot-pressed in air at 1650 ± 20° C

Material		Hot-pressing time (min)							
		3	5	15	20	25	30	35	40
A	G.D. (Mg m^{-3})	1.74	1.78	1.77	1.75	1.78	1.80	1.80	1.80
	H.D. (Mg m^{-3})	2.84	2.88	2.93	2.93	3.02	3.05	3.10	3.00
	ΔD (Mg m^{-3})	1.10	1.10	1.16	1.18	1.24	1.25	1.30	1.20
	ΔP	63	62	66	67	70	69	72	67
	% T. D.	89	90	92	92	94	95	97	94
B	G.D. (Mg m^{-3})	1.85	1.85	1.85	1.85	1.85	1.85	1.85	1.85
	H.D. (Mg m^{-3})	2.27	2.39	3.07	3.09	3.10	3.19	3.20	3.21
	ΔD (Mg m^{-3})	0.42	0.54	1.22	1.24	1.25	1.34	1.35	1.36
	ΔP	23	29	66	67	68	72	73	74
	% T.D.	69	73	93	94	94	97	97	98

G.D. = green density.
H.D. = Hot-pressed density.
ΔD = Change in density.
ΔP = Percentage change in density.
% T.D. = Percentage theoretical density.

TABLE II (b) Macrohardness (kg mm^{-2})

Material	Hot-pressing time (min)							
	3	5	15	20	25	30	35	40
A	2099 ± 92	1962 ± 47	1831 ± 106	1952 ± 60	1879 ± 23	2156 ± 286	2100 ± 286	2157 ± 97
B	374 ± 20	792 ± 66	1828 ± 82	1858 ± 60	1892 ± 90	1892 ± 60	2007 ± 74	1962 ± 25

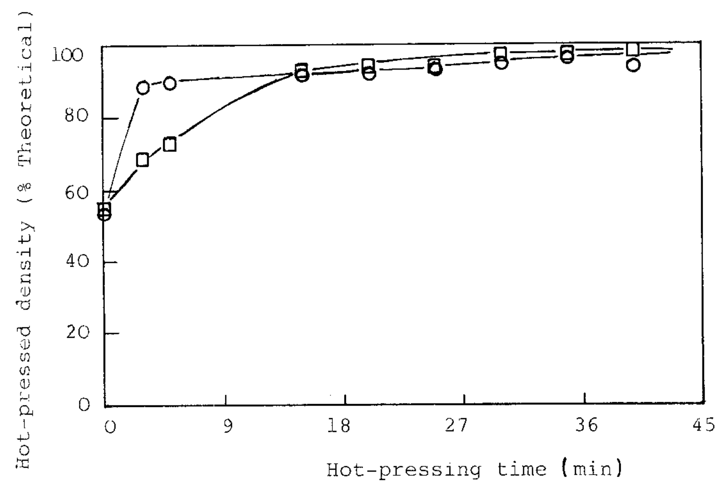

Figure 1 Effect of hot-presing time on hot-pressed density for silicon nitride, hot-pressed with Y_2O_3 and MgO additions. (●) Material A, (□) Material B.

pressure, t is the hot-pressing time and K is a constant. It is seen that the densification is relatively independent of the silicon nitride composition at the later stage of hot-pressing.

Fig. 3 shows the plot of macrohardness value as a function of hot-pressing time. Higher macrohardness values were observed for Material A at the initial time of hot-pressing (3 to 5 min) whilst for Material B, the macrohardness increased more gradually with increase in hot-pressing time.

3.1.3. Effect of temperature on hot-pressing behaviour

The effect of increased hot-pressing temperature in the range 1450 to 1700° C on bulk density, hardness, open and closed pore volume and on the $\alpha \rightarrow \beta$ conversion are given in Tables III and IV, respectively and shown diagrammatically in Figs 4 to 7. Density was found to increase with temperature up to 1650° C but a density decrease was observed for all samples hot-pressed at 1700° C; this decrease is believed to be associated with volatilization of the densification aids at this temperature. Shrinkage was observed to increase with temperature for all hot-pressed (Fig. 6) samples whilst pore closure was maximum at 1650° C followed by a slight increase in pore volume at 1700° C (due probably to the volatilization effects).

Hardness was also found to increase with temperature (Fig. 5). The $\alpha \rightarrow \beta$ phase transformation was observed to be independent of hot-pressing temperature up to 1560° C; a transition occurred in the temperature range 1560 to 1600° C and complete conversion to β-phase was achieved by hot-pressing above 1620° C (Fig. 7).

3.1.4. Microstructure

The microstructure of the hot-pressed specimens are shown in Fig. 8. For Material A, an equiaxed grain distribution was observed with a few occasional tabular primary grains.

The intergranular phase is the residual of a liquid phase (arrowed). For Material B, a bimodal grain distribution was found, consisting of a mixture of elongated (tabular) and equiaxed grains. The morphology of the grains was observed to be related to the temperature of hot pressing, grain globularization was observed in the samples hot pressed at 1700° C (Fig. 8) due to partial solution (on particle periphery) by

TABLE III Results of hot-pressing of silicon nitride at 14 MPa for 30 min. T.D. = theoretical density

Material	Consolidation temperature (° C ± 20° C)	Bulk density		Macrohardness ($kg\,mm^{-2}$)	Open porosity (%)	Closed porosity (%)
		($Mg\,m^{-3}$)	(% T.D.)			
A	1450	2.01	(63)	509 ± 39	30.3	6.7
	1550	2.46	(77)	638 ± 86	14.4	8.6
	1650	3.06	(95)	2156 ± 286	0.48	4.5
	1700	2.85	(89)	2167 ± 260	5.1	5.9
B	1450	2.14	(65)	208 ± 6	34.0	1.0
	1550	2.41	(73)	1028 ± 68	22.9	4.1
	1650	3.19	(97)	1892 ± 60	0.8	2.2
	1700	3.03	(92)	2091 ± 91	2.7	5.3

TABLE IV Shrinkage and amount of β-phase formed in silicon nitride, hot-pressed at 14 MPa for 30 min

Material	% Change at							
	1450 ± 20° C		1550 ± 20° C		1650 ± 20° C		1700 ± 20° C	
	$\Delta V/V_0$	β	$\Delta V/V_0$	β	$\Delta V/V_0$	β	$\Delta V/V_0$	β
A	25.6	36(+3)	32.2	44(+11)	45.9	100(+67)	47.0	100(+67)
B	15.2	39(+25)	27.0	43(+29)	45.3	100(+86)	45.5	100(+86)

(+) increase in beta phase after hot-pressing.

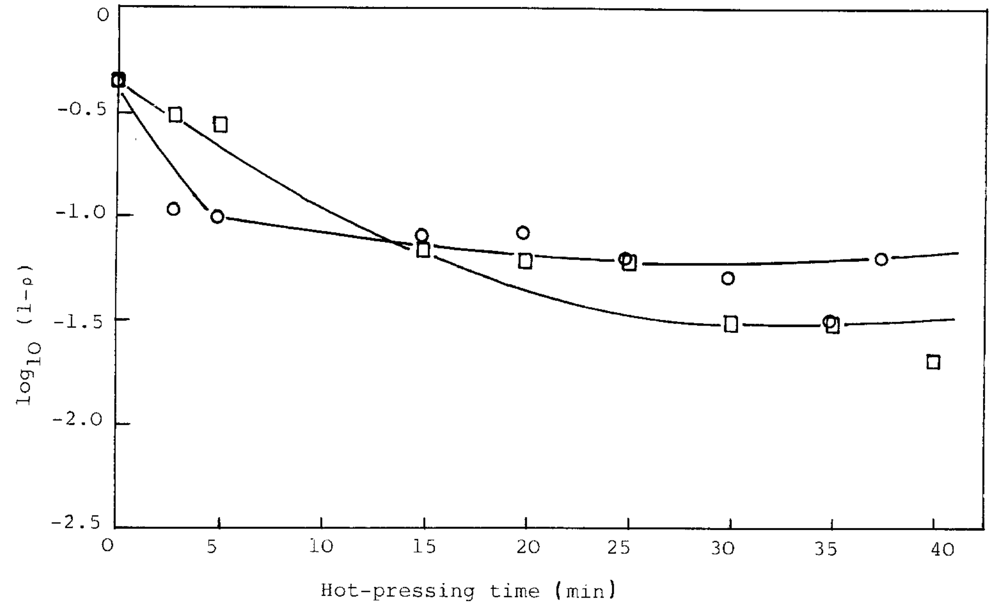

Figure 2 Correlation between log $(1 - \varrho)$ and time for silicon nitride compacts hot-pressed at 1650° C. (○) Material A, (□) Material B.

reaction with the liquid phase; this was not evident in the samples hot-pressed at lower temperatures (1450 to 1650° C).

Residual porosity composed of approximate spherical pores with diameter $< 1\,\mu$m was uniformly (intergranularly) distributed in most materials.

3.2. Fracture strengths

The fracture strengths were calculated using the relation for the diametral-compression disc test

$$\sigma_f = \frac{2P}{\pi d t} \qquad (2)$$

where σ_f is the fracture strength (MPa), P is the load at fracture, d and t are, respectively, the diameter and thickness of the test specimen; the results are given in Table V. It is seen that Material A has a higher average fracture strength than Material B (Material A: 174 ± 32 MPa and Material B 128 ± 14 MPa). The dispersion of the fracture strength values which is given by the standard deviation is lower for Material B and the coefficient of variation (which provides a normalized measure of the dispersion of the fracture strength values) is also lower for Material B. The results are presented as histograms in Fig. 9.

4. Discussion

4.1. Effect of powder composition on densification behaviour

Some degree of densification by particle rearrangement was achieved for both materials when they were cold-pressed before heat-treatment. The green

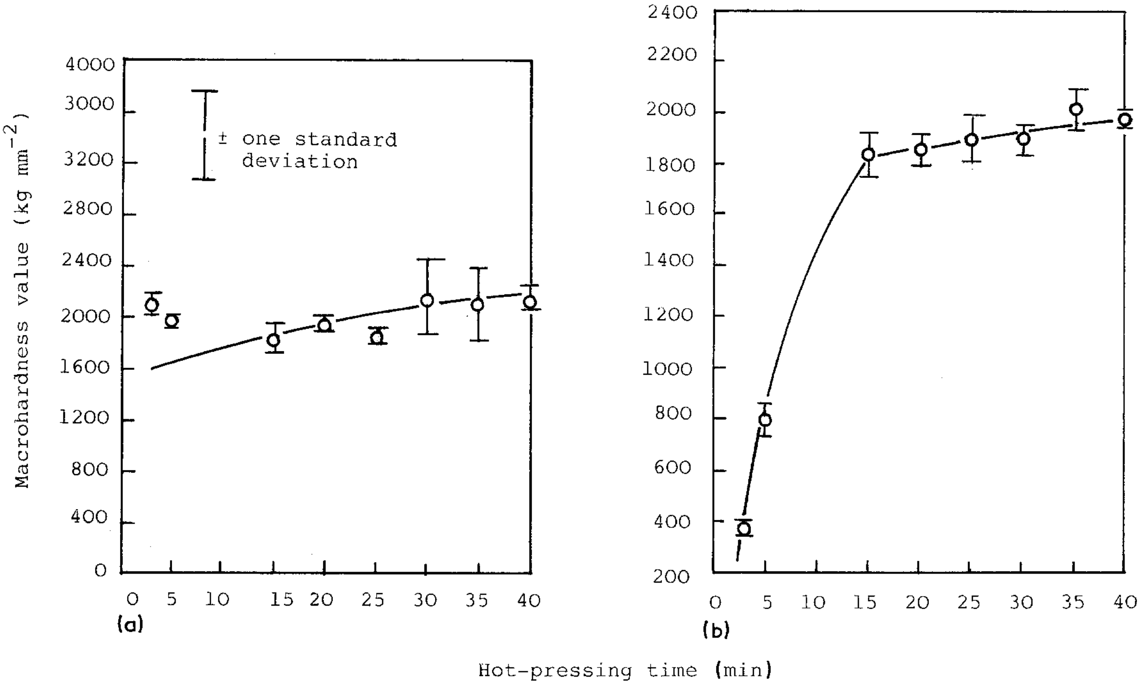

Figure 3 Macrohardness values and hot-pressing time curves for silicon nitride with Y_2O_3 and MgO at 14 MPa and MgO additions at 14 MPa and 1650° C. (a) Material A, (b) Material B.

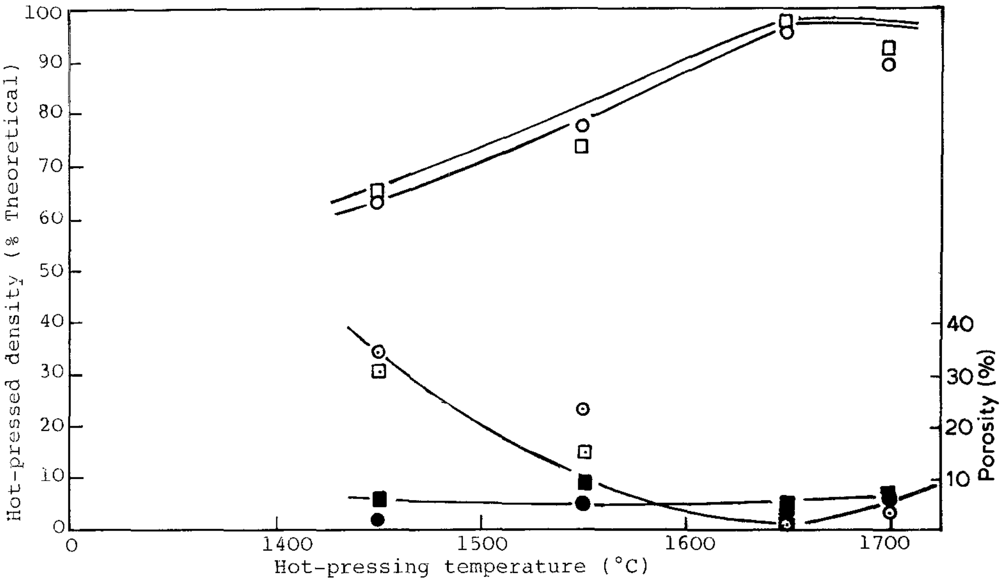

Figure 4 Typical hot-pressed density, porosity and temperature curves for hot-pressed silicon nitride with Y_2O_3 and MgO additions. Material A, 5 wt % MgO, (□) open pores, (■) closed pores. Material B, 2 wt % MgO + 10 wt % Y_2O_3, (○) open pores, (●) closed pores.

densities for the two compositions do not differ significantly. Composition A (5 wt % MgO) has an average green density of about 54% and Composition B (2 wt % MgO + 10 wt % Y_2O_3) has about 55% theoretical density.

The effect of hot-pressing time on densities (Fig. 1) shows that increasing densities with increase in hot-pressing time were generally observed for both materials and this increase was observed to be composition dependent. Densification was much more rapid for Material A but a drop in density was observed after 40 min hot-pressing at 1700° C; this drop in density is due partly to grain globularization (Fig. 8) and volatilization of the liquid phase. For Material B, densification was much more gradual at the initial stage of hot pressing but higher densities were generally achieved with this material.

The effect of the applied pressure on densification was considered in terms of the pressure–density relationship which was originated by Felten [4] and used by Kingery *et al.* [5] for hot-pressed copper–bismuth compacts (Fig. 10). In both cases a poor correlation exists between experimental data and the predicted behaviour according to Equation 1 (which is phenomenologically based) which would predict an initial period of rapid consolidation followed by "plastic flow" behaviour. It is seen that the function of the liquid phase (in the current work and the copper–bismuth work reported by Kingery *et al.*) is to increase the densification that occurs during the initial stages of pressing; the later stages of the densification process, corresponding to plastic deformation of the grains, is essentially independent of the presence of the liquid phase. Unlike Kingery's results, in this work grain deformation was not evident in the hot-pressed samples because of the lack of plastic deformation processes in silicon nitride.

TABLE V Room-temperature fracture strength for hot-pressed silicon nitride (1650° C, 14 MPa, 30 min)

	Material A, σ_f (MPa)	Material B, σ_f (MPa)
Average	174 (10)	128 (10)
Standard deviation	±32	±14
Coefficient of variation (%)	18	11

Number of specimens tested in brackets.

4.2. Hardness measurements

In common with most mechanical properties of brittle materials, a large variability is often observed in measured hardness values [1]. Another feature common to these materials is that the hardness value varies with applied load: the smaller the applied load the higher the hardness value [1, 6]. This behaviour is believed to be related to the fracturing of the crystals; light loads rarely fractured large crystals whilst large loads fractured large crystals and increased the depths of penetration and indentation size.

Macrohardness values plotted as a function of hot-pressing time (Fig. 3) show an increase in macrohardness value with increase in hot-pressing time. Lower values were generally recorded for Material B at

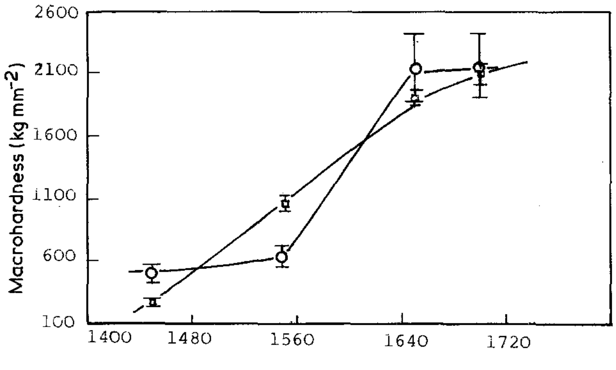

Figure 5 Macrohardness against temperature curves for hot-pressed silicon nitride with Y_2O_3 and MgO additions (○) Material A; (□) Material B.

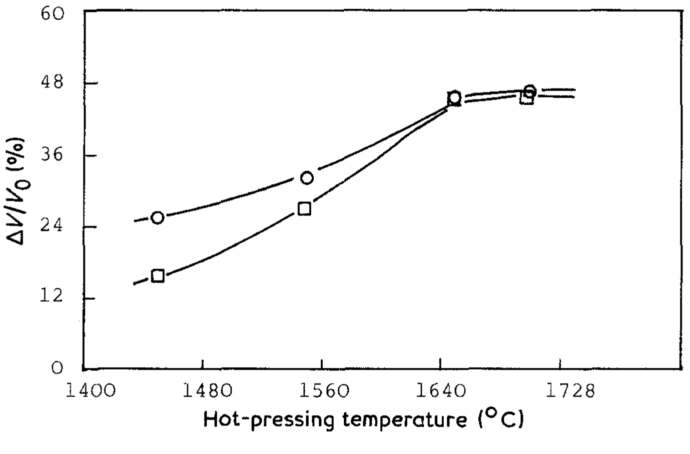

Figure 6 Shrinkage after 30 min at various hot-pressing temperatures for silicon nitride with Y_2O_3 and MgO additions. (○) Material A, (□) Material B.

shorter times of hot-pressing (typically 3 to 5 min); this range of moderately low hardness values (374 to 794 kg mm^{-2}), indicated poor bonding in specimens which had densities of 62 to 74% theoretical. The microstructural observations indicate that this level of density was achieved predominantly by particle rearrangement and fragmentation, without the development of a new grain structure, i.e. there were no distinct grain-boundary structures. Generally the measured hardness values (374 to 2157 kg mm^{-2}) were higher than previously reported [7, 8] (with undefined loads) and confirmed that good bonding was achieved. The scatter in the hardness results is consistent with the published work of Deeley [7], Prochazka and Rocco [9] and others [6].

4.3. Effect of temperature on hot-pressing behaviour

Figs 4 to 7 shows the effect of temperature on the densification of silicon nitride after 30 min pressing for the two materials; the $\alpha \rightarrow \beta$ transformations are also shown (Fig. 7). For Material A (with MgO) the initial liquid formation at 1390° C [1] is accompanied by a rapid increase in density. Densification continues to a relative density of 95% at about 1650° C and this is achieved with an open porosity of less than 1%. The density was found to decrease at 1700° C to a relative density of 89% with an open porosity of 5.1%. With the yttria (Y_2O_3) system, initial liquid formation occurs at 1480° C [1] followed by a rapid increase in density. Densification continues at about 1650° C to a relative density of 97% with an open porosity of about 3%; at 1700° C the relative density dropped to a value of 92% with an open porosity of about 5.3%. This density variation was observed in both materials, an initial increase in density followed by a drop at ~1700° C. This is thought to be related to the volatilization of the liquid phase at 1700° C; the

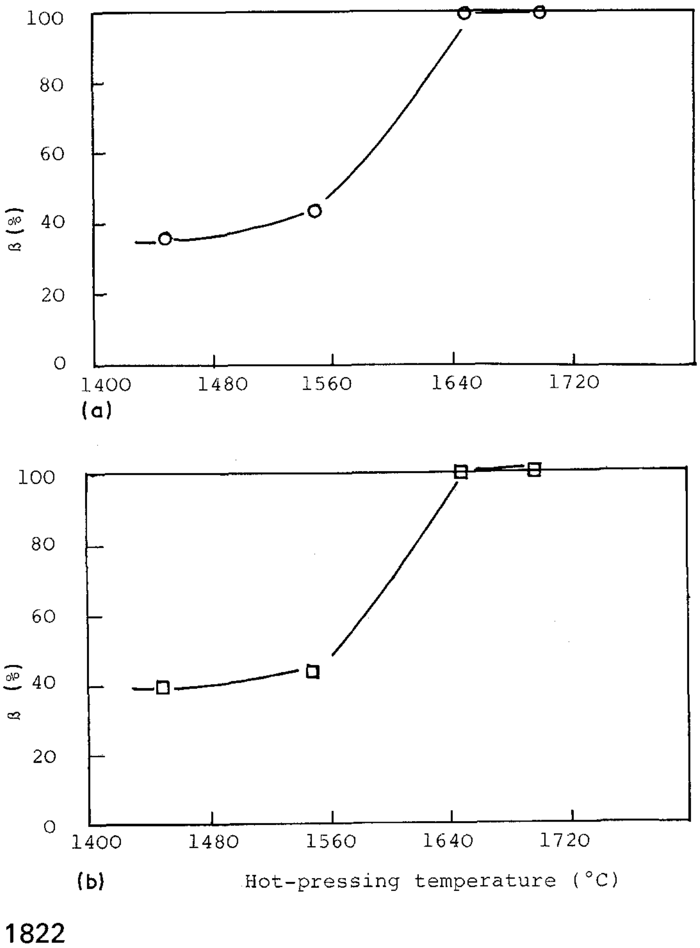

Figure 7 % β-Si_3N_4 after 30 min at various hot-pressing temperatures, (a) Material A, (b) Material B.

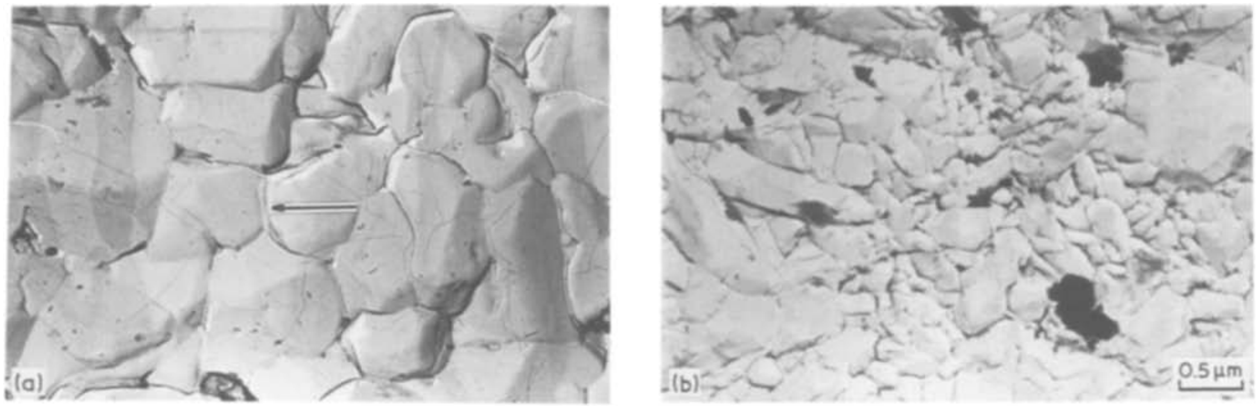

Figure 8 Transmission electron micrographs of polished and etched samples of the hot-pressed silicon nitride with MgO and Y_2O_3 additions. (a) Material A, showing equiaxed grain structure, the intergranular phase is probably the remains of a liquid phase (arrowed), and (b) Material B, showing a bimodal grain structure (small back spots are artefacts on replica). Large black areas are grains that adhered to replica.

increase in the open porosity, at this temperature level is consistent with such an effect. Another factor which might contribute to this drop in density at 1700° C is non-uniform grain globularization (and the associated porosity).

Most of this shrinkage commenced at the temperature of liquid formation and was subsequently accompanied by the $\alpha \rightarrow \beta$ transformation. The shrinkage/temperature and β-phase/temperature curves (Figs 5 to 7) show that shrinkage increases with hot-pressing temperatures to about 1650° C after which no noticeable change was observed at about 1700° C. In this latter stage, grain coalescence and growth occurs in preference to further densification.

The extent of the $\alpha \rightarrow \beta$-phase transformation did not affect the densification processes significantly, in accord with previous reports [1, 10, 11].

4.4. Fracture strengths

The arithmetic mean of the fracture strengths listed in Table V shows that the room-temperature fracture strength for Material A is greater than that for

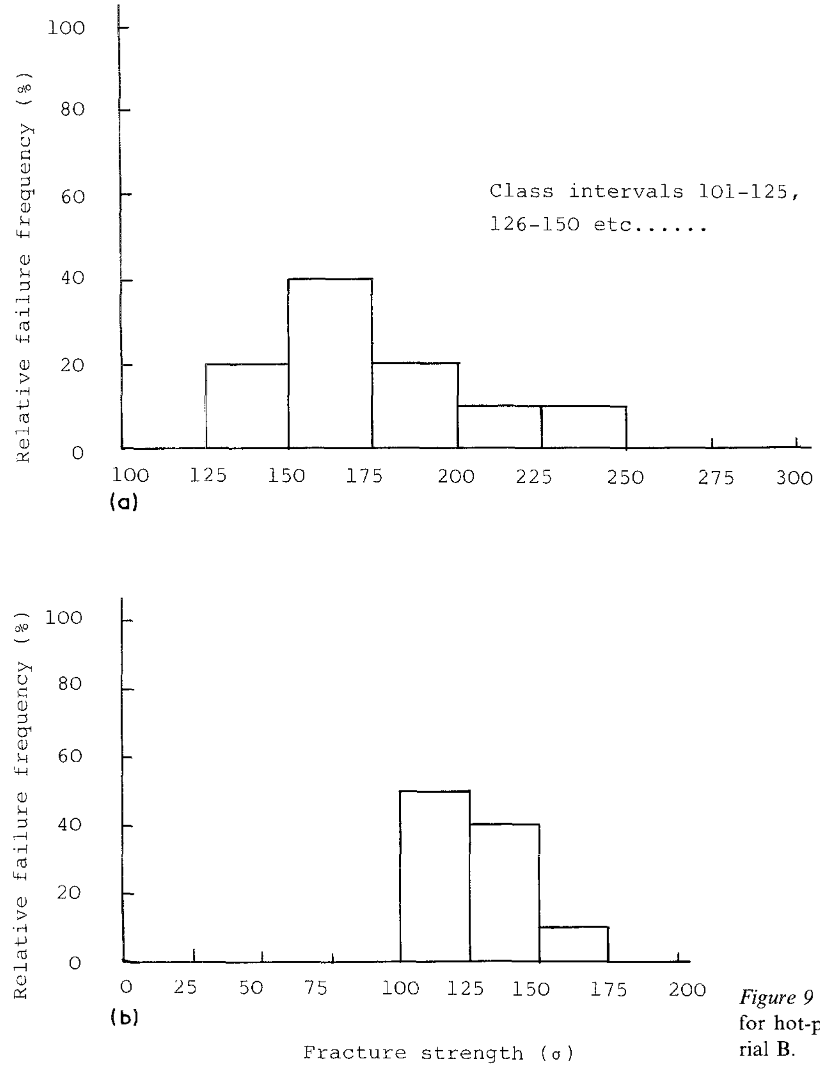

Figure 9 Room-temperature fracture strength distribution for hot-pressed silicon nitride, (a) Material A, (b) Material B.

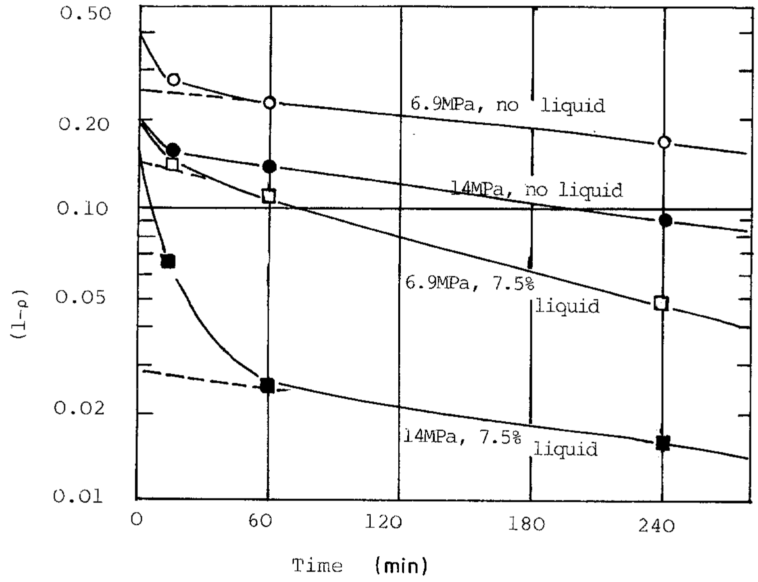

Figure 10 Correlation between $\log(1-\varrho)$ and time for copper–bismuth compacts hot-pressed at 600° C according to Kingery *et al.* [5].

Material B (Material A: 174 ± 32 MPa, Material B: 128 ± 14 MPa). However, the spread of the fracture strength is more for Material A (indicated by the standard deviations and coefficient of variations); the implication of this is that Material B would be preferred for conditions where less scatter of fracture strength is required, whilst Material A would be preferred where a high room-temperature fracture strength was required.

The significance of the differences in fracture strength between the two compositions was evaluated using Wilcoxon's sum-of-ranks' test [1, 12, 13]. The non-parametric procedure, which avoids arbitrary assumptions about the form of the strength distribution, is used to test the null hypothesis that the two data compared are drawn from populations having the same mean. The probability was found to be $\leqslant 2.5\%$ [1] that the null hypothesis was correct for the two materials, i.e. the difference between the fracture strength of the two compositions is statistically significant.

This fracture strength difference is directly related to the compositions of the two materials. Because the additives are intergranularly distributed after hot-pressing, the mechanical properties of these materials would depend on the grain-boundary phases. Whereas it is unlikely for failure to be initiated within the relatively hard silicon nitride grains, the grain boundaries, possibly containing the remnants of a liquid phase, are likely crack sources.

5. Conclusions

1. Two proprietary silicon nitrides containing magnesia (MgO) and a mixture of yttria and magnesia (Y_2O_3 + MgO) were hot-pressed to near theoretical density.

2. The densification rate was dependent on the amount of liquid present which was compositionally controlled; this was confirmed by the densification of Material B (2 wt % MgO + 10 wt % Y_2O_3) which had more liquid phase than Material A. Higher densities were achieved in Material B.

3. The optimum hot-pressing temperature and time at 14 MPa for both materials was found to be ~1650° C and ~30 min. Above this temperature, e.g. 1700° C, a decrease in density, an increase in open porosity and grain globularization occurred, whilst below this temperature (1450 to 1550° C) little densification was recorded because of the lack of transient liquids at these temperatures.

4. The amount and composition of the densification aids directly affect the room-temperature fracture strengths of hot-pressed silicon nitride.

Acknowledgement

The authors thank Dr T. H. Grundy, Turner and Newall Materials Research Limited, for the particle size and the specific surface area analysis.

References

1. J. E. O. OVRI, PhD thesis, University of Manchester (1986).
2. "Focus on Engineering Ceramics", *Metal Powder Rep.* **41** (6) (1986) 476.
3. G. E. GAZZA, *J. Amer. Ceram. Soc. Bull.* **54** (1963) 391.
4. E. J. FELTEN, *ibid.* **44** (1961) 381.
5. W. D. KINGERY, J. M. WOULBROUN and F. R. CHARVAT, *ibid.* **46** (1963) 391.
6. H. C. DUNEGAN, in "Mechanical Properties of Engineering Ceramics", edited by W. W. Kriegel and H. Palmour (Interscience, New York, 1961).
7. G. G. DEELEY, J. M. HERBERT and N. C. MOORE, *Powder Metall.* **8** (1961) 145.
8. D. STEINMAN, "Silicon-Nitride" (Elektroschmelzwerk Kempteum, München, Germany, 1986).
9. S. PROCHAZKA and W. A. ROCCO, *High-Temp. High-Press.* **10** (1978) 87.
10. K. H. JACK, *Mater. Sci. Res.* **11** (1978) 125.
11. R. J. WESTON and T. G. CARRUTHERS, *Proc. Brit. Ceram. Soc.* **22** (1983) 197.
12. F. WILCOXON, *Biometrics* **3** (1947) 119.
13. A. B. BOWKER and G. J. LIEBERMAN, "Engineering Statistics", 2nd Edn (Prentice-Hall, New Jersey, 1972).

Received 5 January
and accepted 4 March 1987